Drifting Diaphyses: Asymmetry in Diametric Growth and Adaptation Along the Humeral and Femoral Length

ISABEL S. MAGGIANO,[1]* COREY M. MAGGIANO,[2,3] VERA G. TIESLER,[4] JULIO R. CHI-KEB,[4] AND SAM D. STOUT[5]

[1]Department of Anatomy and Cell Biology, University of Saskatchewan, 3B36 Health Sciences, Saskatoon, SK, S7N 5E5 Canada

[2]Department of Anthropology, West Georgia University, 1601 Maple Street, Carrollton, Georgia 30118

[3]Department of Anthropology, University of Western Ontario, Social Science Centre Rm 3326, London, Ontario, N6A 5C2 Canada

[4]Department for Anthropological Sciences, Universidad Autónoma De Yucatán, Carr. Mérida Tizimín, Km.1, Mérida, Yucatán, CP, 97305 Mexico

[5]Department of Anthropology, The Ohio State University, 4052 Smith Laboratory, Columbus, Ohio 43210

ABSTRACT

This study quantifies regional histomorphological variation along the human humeral and femoral diaphysis in order to gain information on diaphyseal growth and modeling drift patterns. Three thin sections at 40, 50, and 60% bone length were prepared from a modern Mexican skeletal sample with known age and sex to give a longitudinal perspective on the drifting cortex (12 adults and juveniles total, 7 male and 5 female). Point-count techniques were applied across eight cross-sectional regions of interest using the starburst sampling pattern to quantify percent periosteal and endosteal primary lamellar bone at each diaphyseal level. The results of this study show a posterio-medial drift pattern in the humerus with a posterior rotational trend along the diaphysis. In the femur, we observed a consistent lateral to anteriolateral drift and an increase in primary lamellar bone area of both, periosteal and endosteal origin, towards the distal part of the diaphysis. These observations characterize drifting diaphyses in greater detail, raising important questions about how to resolve microscopic and macroscopic cross-sectional analysis towards a more complete understanding of bone growth and mechanical adaptation. Accounting for modeling drift has the potential to positively impact age and physical activity estimation, and explain some of the significant regional variation in bone histomorphology seen within (and between) bone cross-sections due to differing ages of tissue formation. More study is necessary, however, to discern between possible drift scenarios and characterize populational variation. Anat Rec, 298:1689–1699, 2015.   © 2015 Wiley Periodicals, Inc.

Key words: bone; histology; modeling; drift; primary lamellar bone; tissue age; microstructural variation; diaphysis

Long bone growth and mechanical adaptation requires complex adaptive formation and resorption, leading to dramatic changes in diaphyseal size, shape and curvature. Endochondral and intramembranous ossification extend and expand the bone during growth phases. Growth, the simple net increase in size, can be separated from "modeling," which refers to uncoupled resorption or formation at the periosteal and endosteal surfaces (Frost, 1973; Martin et al., 1998). Periosteal and endosteal modeling of the diaphysis determines a bone's final shape and robusticity (Enlow, 1962; Frost, 1973; Maggiano, 2012b). During these modeling processes, bone is formed in sheets, called lamellae. Primary lamellar bone persists until it is eventually remodeled, or reabsorbed at the periosteal or endosteal membrane to adjust robusticity, curvature, or alter the bone's position relative to joints and neighboring skeletal elements. Modeling drift, also called osseus or cortical drift, defines all positional changes of the diaphysis achieved by modeling processes (Enlow, 1962; Frost, 1973; Goldman et al., 2009; Maggiano, 2012b). The most simple drift scenario consists of periosteal deposition on the leading, and resorption on the lagging drift cortex. In order to maintain the medullary cavity's relative position, the endosteum mirrors the process, with deposition and resorption on the lagging and leading cortices, respectively. This process moves the bone in tissue space, creating curvature along the element or altering orientation. Modeling drift is, however, not necessarily linear but can be curvilinear (normally rotational, Maggiano, 2012b). Regulated by mechanical strain levels, as well as the demands of maintaining vascular continuity and mineral homeostasis, modeling drift maintains a balance between mechanically optimized shape, size, and mass throughout the life of an individual (Martin et al., 1998; Turner, 1998). Once formed, the material integrity of bone is maintained by a process called remodeling. Remodeling is achieved by the coordinated action of osteoclasts and osteoblasts, referred to as Basic Multicellular Units (BMUs) (Martin et al., 1998; Parfitt, 2000). The bone structural units (BSUs) produced by remodeling processes are Haversian Systems, or secondary osteons, cylindrical microscopic structures that tunnel and branch through primary bone. Remodeling of primary bone tissue in long bones starts *in utero* and continues throughout life (Currey, 2003). Modeling and remodeling dynamics leave a stratigraphic pattern consisting of different tissue types that can be microscopically identified and used to reconstruct modeling drift history (Maggiano et al., 2011; Maggiano, 2012a).

Despite the microscopic nature of variation in tissue types, macroscopic analysis has significantly added to our knowledge about diaphyseal growth and adaptation (Ruff and Hayes, 1983; Gosman et al., 2013). Most importantly, animal experiments have demonstrated that cross-sectional shape adaptation is reactive to very high, repetitive loading (Mosley et al., 1997; Mosley and Lanyon, 1998, 2002; Robling et al., 2001). While these experiments show that periosteal expansion can be triggered in a relatively short amount of time, a narrowing of the medullary cavity, indicative of a formative reaction at the endosteal surface, is usually absent (Meade et al., 1984; Jones et al., 1991; Gross et al., 2002). It has therefore been suggested that the endosteum is less responsive to mechanical stimuli than the periosteum.

However, it is difficult to interpret local relative strain differences on each surface and caution must be used in transferring observations on short-term young animal models to the human case.

While histological studies on microstructural variation in human long bones have recently become more common (Goldman et al., 2005, 2009; Maggiano et al., 2011; Cambra-Moo et al., 2012, 2014), they rarely address human modeling drift (for exceptions see Goldman et al. 2009; Maggiano et al., 2011; Maggiano, 2012a). Our previous research (Maggiano et al., 2011) used the distribution of endosteal lamellar bone, termed the ELP (Endosteal Lamellar Pocket), in the midshaft femur of adult archaeological individuals as an indicator of the direction of modeling drift and identified a dominantly lateral drift pattern. It provided results consistent with Goldman et al.'s, (2005) study indicating that primary endosteal bone in the femur has constant positional characteristics and is present in individuals up to at least 55 years of age. In addition, Goldman et al. included more sub-adult individuals, and they report drift to be posterior and medial at the midshaft femur in toddlers, shifting anteriolaterally in late childhood (Goldman et al., 2009). While the human humerus is less frequently used for histological analysis, a recent study by Cambra-Moo et al., (2014) gives detailed information about regional tissue type distribution and relative degrees of mineralization. The authors do not directly relate their findings to drift patterns, but their results support the posterio-medial humeral drift suggested by Maggiano (2012a). Interestingly, this drift pattern seems to be consistent even with nonhuman primate species as McFarlin et al. (2008) suggest for *Chlorocebus aethiops*, *Hylobates lar* and *Pan troglodytes* in their analysis of the distribution of secondary tissue. A study by Paine and Godfrey (1997) also compared the regional variation of secondary tissue in three cross-sections along the humeral and femoral diaphysis, similar to this study. The authors found the humerus of several quadrupedal primate species showed higher remodeling rates than the femur, while specialized leapers showed the opposite pattern, suggesting a relationship between remodeling rate and locomotor behavior (primates used in this study belonged to the families Galagonidae and Cercopithecidae). Regional variability of secondary bone tissue across proximal, midshaft and distal sections of the humerus and the femur was similar across different locomotor types (Paine and Godfrey, 1997).

Despite collecting a growing amount of information on bone growth, adaptation, and the regional distribution of tissue types in long bones, little is known about drift direction, magnitude and variability along diaphyses. Moreover, drift is not necessarily uniform along the shaft. Complex positional changes and necessary curvature achievements in combination with the simple fact that long bones are attached through joints at both ends could require drift to be rotational and/or differ in magnitude along the shaft. In addition, modeling could react differently to systemic and local factors in weight-bearing versus nonweight bearing bones. For these reasons, the present investigation quantifies the distribution of periosteal and endosteal primary lamellar bone within three cross-sections along the human humerus and femur in order to interpret these distributions in

terms of modeling drift patterns. Net diaphyseal growth can be observed in living specimens through clinical CT or X-ray; however, the details of how modeling is achieved are only available through microscopic sampling. Due to tradeoffs between resolution and volume of interest in micro CT, only optical microscopy permits quantitative or even qualitative analyses of regional distributions of large primary bone deposits. For these reasons, we employed histological point-count techniques in a star-burst pattern (Maggiano, 2012a), which permits a statistical analysis of bone type distributions across regions of interests within transverse cross-sections and between one or more sections along the humeral and femoral diaphysis. In this way, the present study provides information about drift along the diaphysis, the nonweight-bearing humerus and the weight-bearing femur.

MATERIAL AND METHODS

Individuals used in this study are part of a reference collection from the urban cemetery Xoclán, Mérida, Yucatán (Chi-Keb et al., 2013). It is curated at the Universidad Autónoma de Yucatán, Mexico (made available for investigation with permissions from the Municipal Government of Mérida) and consists of 84 individuals who were born between 1900 and 1990 and died between 1995 and 2004. The sample provides a frame of reference for archaeological sites in the same region, making this an important and unique skeletal collection.

All individuals between 8 and 45 years at death were selected for sampling (N = 14). The bottom of the range is determined by the youngest individual available in the sample. Individuals over the age of 45 years were excluded because of age related diaphyseal changes and the decreased likelihood of the presence of primary lamellar bone (due to continuous remodeling and age-associated bone loss) (Maggiano et al., 2011). During analysis, two more individuals were excluded from the sample, the first due to pathological changes at the endosteum (nonspecified woven bone formation along the medullary cavity). The second (an 8-year-old female) was removed from the sample because of results reported by Goldman et al. (2009) indicating that regional variation of primary bone deposits are more consistent after the age of 12. The final sample includes seven males (mean age-at-death = 33.4 ± 8.5; age range, 18–45) and five females (mean age-at-death = 30.3 ± 11.0; age range, 12–42). All bones included in the study were from the left side; one left humerus was not available and only the femur was used of this individual.

During macroscopic analyses (standard osteometric measurements and screening for pathologies), an anterior line was defined and marked on all humeri and femora used in this study. In the humerus, this line summarizes the positions of the lesser tubercle, the most superior aspect of the brachialis insertion, and the apex of the anterior curve between the lateral and medial supracondylar crest. In the femur, we used the linea aspera as an indicator of the posterior direction. Afterwards, three transverse cross-sectional microscopic slides were prepared from each bone. Maximum bone length was used to determine the midshaft (50%), the proximal (40%), and the distal (60%) section. These diaphyseal positions were chosen to ensure sampled areas
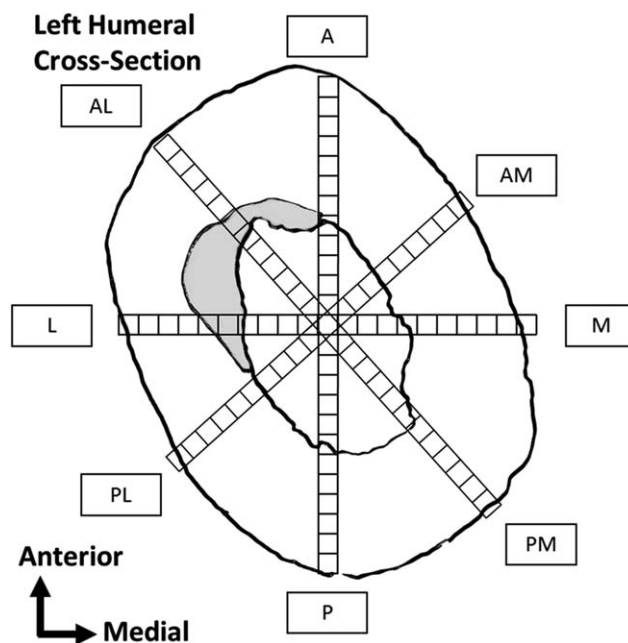

Fig. 1. Representation of the starburst sampling pattern on a humeral midshaft cross-section. The four axes correspond to eight regions of interest (ROIs). A, anterior; AL, anteriolateral; L, lateral; PL, posterio-lateral; P, posterior; PM, posterio-medial; M, medial; AM, anterio-medial.

remained within the diaphysis and trabecular bone was avoided. Three two centimeter blocks were extracted from each bone centered around these locations. Microscopic thin-ground sections were made using Biodur® plastination and hand sanding techniques as described by Schultz (1988) and Schultz and Drommer (1983). After embedding, a 1 mm slice was extracted from each block using a Buehler Isomet Saw. This slice was affixed to a microscope slide, ground down to 70–100 μm, polished and cover-slipped.

The point-count technique was used to capture microstructural variation across the entire cross-section, in a systematic star-shaped pattern (Fig. 1). This starburst sampling strategy includes eight regions of interest (ROIs) defined by the cardinal anatomical axes and halfway points between them [A (anterior), AM (anteriomedial), M (medial), PM posterio-medial, P (posterior), PL (posterio-lateral), L (lateral), AL (anteriolateral)]. First, an anterio-posterior line was marked on the microscopic slide to identify the anterior and the posterior ROI. For this purpose, a line was drawn connecting the most anterior point of the cross-section (as marked on the bone before sectioning) and the centroid. To determine the centroid or geometric center of the cross-section, we used Image J 1.44p and MomentMacro J (Ruff; www.hopkinsmedicine.org/- fae/mmacro.htm). All other ROIs (anteriolateral, lateral, posterio-lateral, posterio-medial, medial, and anterio-medial) could be identified afterwards, through lines forming 45° angles with the anterio-posterior line.

Periosteal and endosteal primary lamellar bone was differentiated on the basis of vascular and histomorphological traits that can identify the membrane of origin (for details see Maggiano, 2012b). Periosteal and
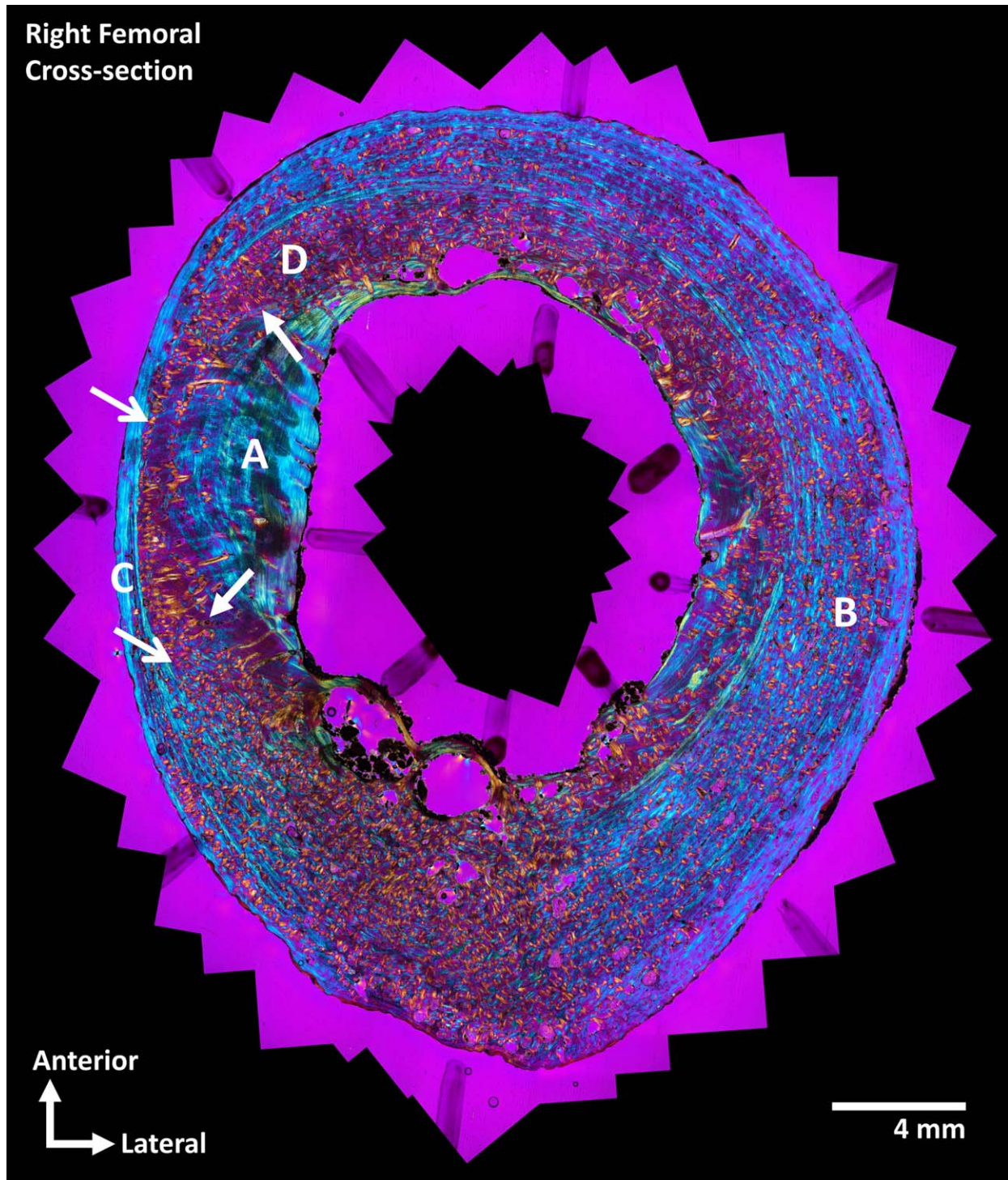
Fig. 2. Micrograph of a complete femoral midshaft cross-section stitched using Autopano Giga®. Each 530 nm compensated image was captured using a cross-polarized 45° technique as outlined in Maggiano et al. (in press) in order to add color-contrast to differing tissue types: secondary Haversian tissue in blue and orange hues and primary lamellar tissue in blue. A) Endosteal primary tissue marks the "wake" of the drifting medullary cavity (solid white arrows denote the intracortical border of endosteal bone populated by secondary osteons). B) Periosteal primary tissue with interspersed secondary osteons and primary canals. C) Periosteal primary lamellar bone marking active appositional growth transpiring after drift cessation (lined white arrows mark the reversal line for the entire diaphysis).
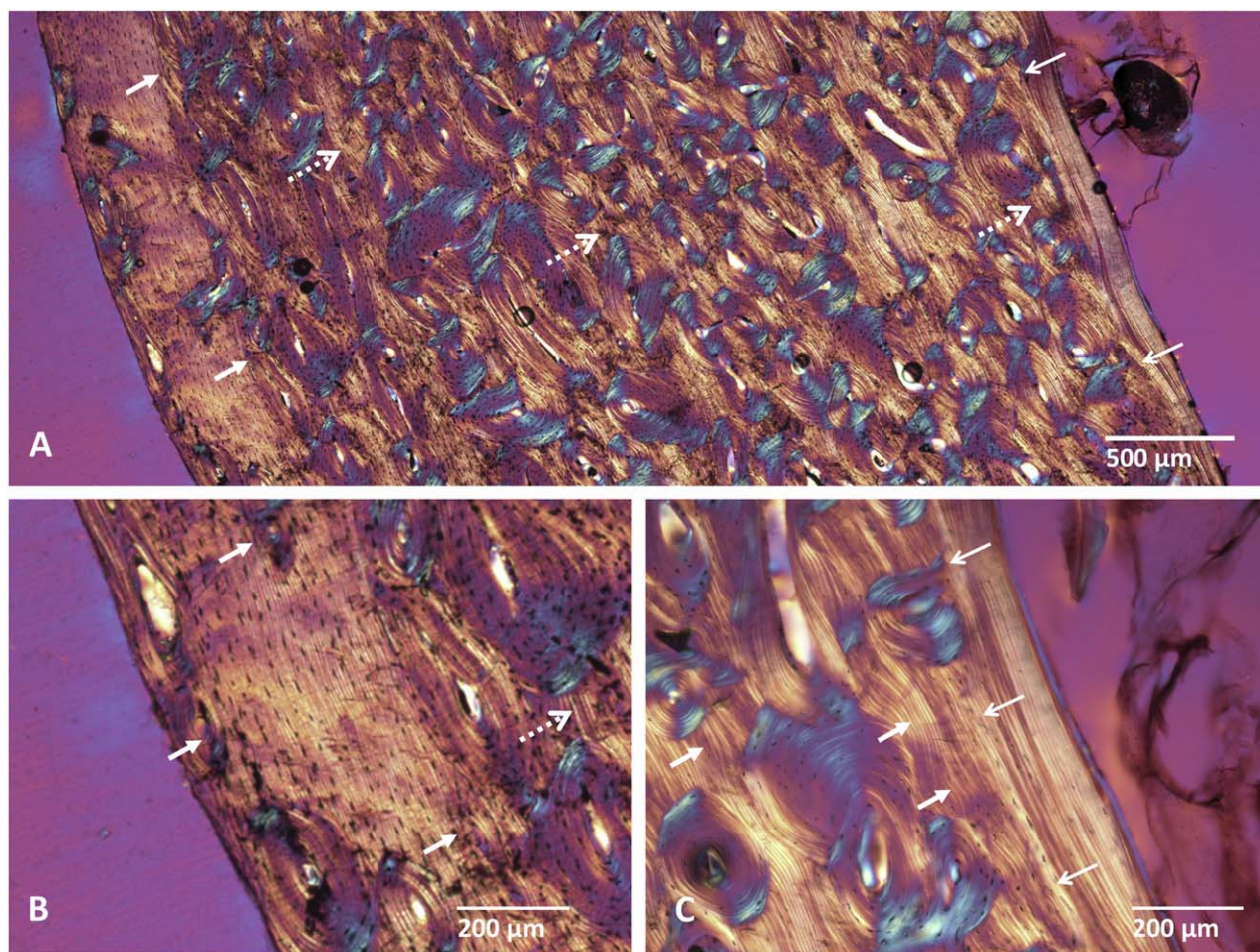
Fig. 3. Stitched micrograph taken using the previously described technique (the golden hue for primary bone is due to photographing the lamella in the opposite orientation). A: Femoral cortex showing the periosteal and endosteal primary lamellar bone and intervening secondary (Haversian) tissue. The periosteum is located at the left side of the image with solid white arrows denoting the newest periosteal layers adjacent to older regions, largely remodeled with interstitial periosteal-origin tissue comprising most of the cortex as marked with dotted white arrows. White lined arrows on the right of the image denote endosteal tissue interfacing with much older periosteal interstitial lamellae. B, C: Details of the exterior and interior cortices showing characteristics of periosteal origin tissue marked with solid arrows, including primary canals in B and their effect on primary periosteal lamellae (waviness) in C. Lined arrows in C show the reversal line of more recent endosteal tissue cutting across primary periosteal lamellae and even partially resorbing some osteons.

endosteal primary lamellar bone show distinctive microstructural characteristics resulting from differing means of vessel entrapment during deposition. Vessels in human periosteal primary bone are typically longitudinal and are referred to as "primary canals" or sometimes "primary osteons," since they can form concurrently with surrounding primary bone (Parfitt, 1983). These primary canals do not require previous resorption, but instead are "sandwiched" between primary lamellae and only have a few lamellae themselves, if any (Maggiano, 2012b). In contrast, endosteal lamellar bone is characterized by radially oriented primary Volkmann canals which extend during growth to ensure a maintained connection between deeper bone tissue and the medullary vascular network (Enlow, 1962; Maggiano et al., 2011; Maggiano, 2012b). This distinctive primary vascularization enables clear identification of periosteal versus endosteal primary bone, especially when combined with polarized light microscopy which enhances lamellar structure (Figs. 2 and 3).

The following microscopic variables were counted at $100\times$ magnification using a 1 mm^2 Merz grid in each ROI. Each counting reticule intersection equals one hit. Total number of hits was documented per ROI for the following variables: (1) sampled bone, (2) periosteal lamellar bone, (3) endosteal lamellar bone. Periosteal and endosteal membrane deposition were standardized by the total number of sampled hits per region of interest for statistical analyses and presentation. Data were non-normal in distribution; a One-Way-Anova Kruskal-Wallis test was used for a comparison between diaphyseal sections, and a Friedman Test was used for between ROI comparisons within single cross-sections. All statistics were calculated using the statistics package SPSS 19. Significance level was chosen at $P < 0.05$.

TABLE 1. Friedman Test to test for significance of variation between all eight regions of interest per cross-section.

	Periosteal	Endosteal
Humerus (N = 11)		
Proximal	**0.000**	**0.001**
Midshaft	**0.000**	**0.022**
Distal	**0.000**	**0.000**
Femur (N = 12)		
Proximal	**0.000**	0.486
Midshaft	**0.000**	**0.000**
Distal	**0.000**	**0.000**

Values in bold type are significant at P < 0.05.

RESULTS

In each of the three humeral cross-sections, proximal, midshaft, and distal, percent periosteal and endosteal primary tissue is significantly different when all eight anatomical ROIs are compared with each other (Friedman Test, see Table 1, Fig. 4). Overall, percent periosteal primary bone is highest in the posterior half of the cortex, while percent endosteal primary bone is highest in the anterior half. Kruskal-Wallis test for comparison of percent periosteal and endosteal lamellar bone between proximal, midshaft and distal (per ROI), shows that periosteal primary bone has significant longitudinal differences in the anterior, posterior, posterio-lateral and lateral region of interest (Table 2, Fig. 4). In the proximal section, primary periosteal bone shows its highest percentage in the posterio-medial region. In both, the midshaft and distal section, the highest percentage of periosteal primary tissue is found in the posterior region. Longitudinal differences of percent endosteal primary tissue are only statistically significant in the medial ROI (Table 2). However, proximally, endosteal primary tissue wraps around the entire anterior and medial half of the medullary cavity. In the midshaft and distal cross-sections, its highest percentage shifts towards anteriolateral, and is especially high for this ROI in the distal cross-section. In summary, both primary tissues, periosteal and endosteal, "shift" toward each other—into the medial cortex—in the proximal cross-section. In contrast, they directly oppose one another in the distal part of the humeral diaphysis.

As in the humerus, Friedman test results show that percent periosteal and endosteal lamellar bone area in the femur show statistically different percentages within proximal, midshaft, and distal cross-sections, when the eight ROI are compared with each other (Table 1, Fig. 5). One exception to this is endosteal primary bone area in the proximal femur. In general, this type of bone was rare in this section of the diaphysis. The femur shows a strong increase in percent primary bone area from proximal to distal. This could be statistically confirmed by Kruskal-Wallis test results (Table 2, Fig. 5), showing significant differences for endosteal lamellar bone area for all but one (anterior) ROIs. A longitudinal trend is also present for periosteal lamellar bone in the femur, although less obvious, and is only statistically significant for the anterior region of interest. The position of primary periosteal and endosteal bone along the femoral diaphysis is similar along the diaphysis, with highest percentages
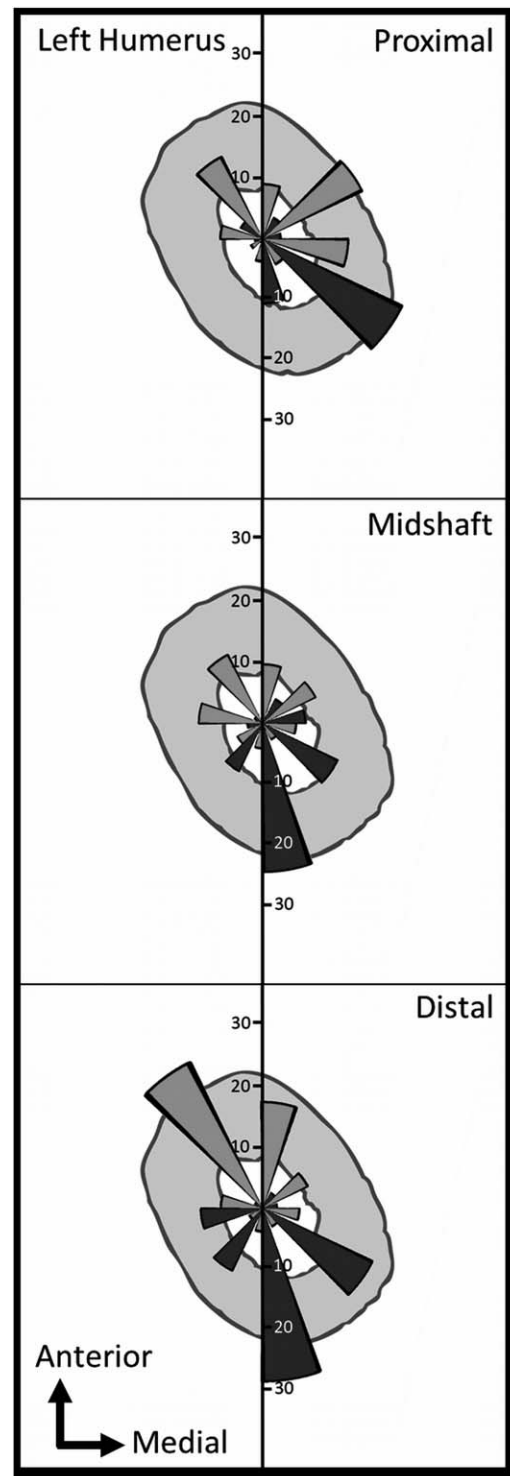

Fig. 4. Percent periosteal and endosteal membrane deposition by region across the humeral proximal, midshaft, and distal cross-sections. Black: periosteal tissue, gray: endosteal tissue.

of femoral periosteal lamellar tissue located in the anterio-medial and anterior ROI, and, mirroring that, highest percentages of endosteal primary tissue located in the posterio-lateral, posterio-medial, and medial ROI.

TABLE 2. Kruskal-Wallis Test for differences between proximal, midshaft and distal sections per bone tissue and region of interest.

	Humerus (N = 11)		Femur (N = 12)	
	Periosteal	Endosteal	Periosteal	Endosteal
Anterior	**0.011**	0.085	**0.017**	0.803
Anterio-medial	0.395	0.078	0.494	**0.049**
Medial	0.248	**0.034**	0.468	**0.000**
Posterio-medial	0.527	0.700	0.296	**0.000**
Posterior	**0.013**	0.924	0.755	**0.000**
Posterio-lateral	**0.000**	0.252	0.503	**0.000**
Lateral	**0.018**	0.502	0.301	**0.000**
Anteriolateral	0.763	0.209	0.031	**0.035**

Values in bold type are significant at $P < 0.05$.

DISCUSSION

This study uses the starburst pattern point-count technique (Maggiano, 2012a) to quantify the distribution of periosteal and endosteal primary bone in three microscopic cross-sections along the diaphysis. Because these tissues are deposited sequentially, their stratigraphy records important aspects of growth and mechanical adaptation. For example, when the distribution of periosteal and endosteal bone oppose one another, a linear drift trend is in effect. Previously reported drift patterns for both the humerus and the femur could be generally confirmed. However, our study also reveals details that are only visible when several sections along the diaphysis are taken into account. In the humeral diaphysis, an interesting rotational trend in drift direction is uncovered, while the femoral drift pattern is characterized by a significant change in primary bone area along its diaphysis. These results emphasize the value of considering both longitudinal and cross-sectional microscopic variation when analyzing long bone growth and modeling drift.

Humerus

Our results confirm a general posterio-medial drift in the human humeral diaphysis described earlier during analysis of only the midshaft (Maggiano, 2012a). This drift pattern can also be seen in images and results from Cambra-Moo et al., (2014), although the authors do not discuss it specifically. A posterior-medial drift seems to be consistent across different primate species - leapers, quadrupeds as well as bipedal humans, as our study combined with others (McFarlin et al., 2008), suggests. This indicates that its general pattern is independent from specific locomotor behavior and points to a strong growth/development component.

Although others have reported similar distributions of primary bone tissue and modeling trends for the midshaft humerus, this is the first occasion where variation in drift has been assessed along the diaphysis. Total area of drifted bone is similar on all three humeral diaphyseal levels, indicating that the entire element is drifting rather than just an aspect initiating curvature or positioning. However, our interpretation of modeling drift notes important deviations from the linear drift scenario. In the proximal part of the humeral diaphysis, both periosteal and endosteal lamellar bone deposits are positioned within the medial half of the cortex. Instead of a drifting mechanism, this pattern of modeling would

cause the medial cortex to thicken. The present study does not analyze histomorphological variation related to muscle insertion, but it is interesting to note that this thickening of the cortex in the proximal humerus is opposite the largest insertion site of the diaphysis (deltoid tuberosity), which lays partly within the 40% section of the diaphysis. While enthesial changes are commonly used in the anthropological literature to reconstruct activity patterns of past populations (Hawkey and Merbs, 1995; Molnar, 2006), little is actually known about the effect of muscle attachment and tension on local bone apposition or microstructural changes (Hoyte and Enlow, 1966). Schlecht (2012) shows increased secondary remodeling in the human radius that he relates to axes of mechanical strain caused by insertion sites, however, the author does not analyze changes in primary lamellar bone. Periosteal lamellae are interrupted at muscle insertion sites, where instead Sharpey's fibers are present, preventing or slowing "normal" periosteal lamellar bone apposition (Carpenter and Carter, 2008). Therefore, theoretically, the humeral proximal diaphysis could respond to increased mechanical strain on the deltoid attachment by adding to its opposite cortex (Maggiano, 2012a). However, future studies are necessary to better understand the relationship between periosteal expansion and muscle insertions and the impact muscle forces have on a bone's modeling activity.

In contrast to the proximal humerus, periosteal and endosteal primary tissues directly mirror each other in the midshaft and distal aspects showing a pattern expected for typical linear diaphyseal drift. Related to the differences in regional primary bone deposits along the humeral diaphysis could be the comparatively large torsion angle characteristic for human humeri (this angle is determined by measuring the angle between the orientation of the humeral head and the distal condyle of the humerus). Torsion is formed through the lateral rotation of the proximal humerus in comparison to the distal part of the bone. In the left humerus, this indicates a "clockwise" twist (Krahl and Evans, 1945; Aiello and Dean, 2002). Our data suggests the largest percentage of periosteal bone rotates from a posterio-medial to a posterior position and the largest percentages of endosteal bone rotate from an anterio-medial to an anteriolateral position. This also indicates a clockwise drift pattern (in the right side this would be counterclockwise, but still mark the rotation from medial to posterior), suggesting a relationship between the
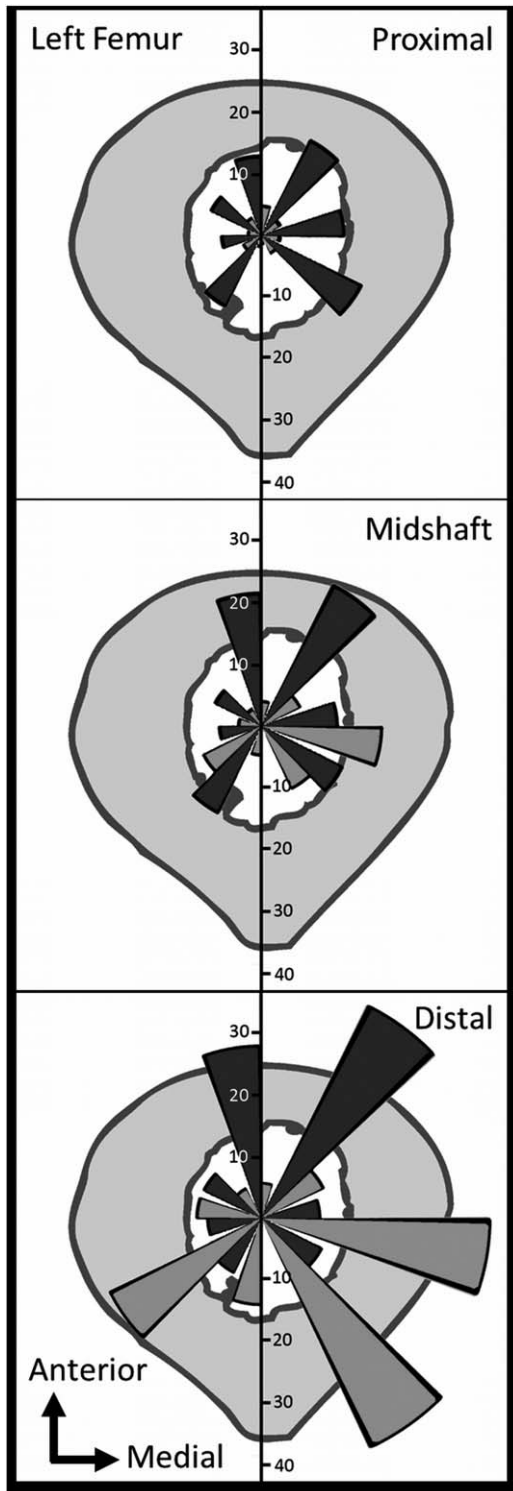
Fig. 5. Percent periosteal and endosteal membrane deposition by region across the femoral proximal, midshaft, and distal cross-sections. Black: periosteal tissue, gray: endosteal tissue.

development of humeral torsion and drift. Humeral torsion does develop early in life, before age 8 (Edelson, 2000), and drift direction has been reported to be more

variable (in the femur) before 12, according to Goldman et al. (2009). However, according to previous work by one of us (Maggiano, 2012a), this could be different in the humerus, where younger individuals also show consistent drift characteristics for the midshaft. Supportive of our suggestion of a relationship between humeral torsion and drift are studies reporting that athletes show a greater torsional angle than non-athletes (Taylor et al., 2009; Whiteley et al., 2009), and athletes practicing movements predominantly causing torsional strain on the bone are on average characterized by larger torsional angles. Specifically in the humerus, as a non-weight bearing bone attached to the rest of the skeleton through the shoulder joint—with the widest range of motion in comparison to other joints—torsional forces are common during many activities. However, caution needs to be practiced in this interpretation since specifically a complex distribution of primary tissue like the one seen in the humerus could also be contributed to or partially obscured by uneven remodeling of the cortex. This issue is particularly cumbersome for comparative analysis of tissues by area comparisons. Interpretations presented here on rotational drift, however, are relatively immune to this concern due to their basis being the changing orientation of primary formation phases.

Femur

Consistent with results reported from previous qualitative studies on the regional distribution of bone tissue types, femoral drift is dominantly lateral with a slight anterior tendency. A posterio-medial drift has been reported for toddlers (Goldman et al., 2005), however, in later childhood, drift becomes consistently lateral. As the present study shows, this drift direction is equal along the femoral diaphysis. There is, however, a strong longitudinal increase of percent periosteal and endosteal lamellar bone towards the distal part of the diaphysis. Many proximal femoral cross-sections contained only small areas of endosteal primary bone, or even none. Also, periosteal primary bone stayed under 20% proximally, in all ROIs. In comparison, both, periosteal and endosteal primary bone average at around 40% in the distal diaphysis. Since a stratigraphic analysis of primary lamellar bone cannot provide information about lamellae that have been resorbed or replaced during continuous remodeling and modeling (Wu et al., 1970), we cannot be sure if our results indicate that the proximal femur experienced less drift, or if primary lamellar bone has been removed during its continuous development. However, considering the strength of the increase of percent primary tissue distally, it is likely that the observed drift pattern is at least partly the result of unequal drift magnitudes. Further study and methodological developments using fluorescence labeling (in non-human animal models) would be necessary to more fully address this question.

Assuming drift magnitude does vary significantly along the femoral diaphysis, several circumstances could potentially explain our observations. In general, femoral cross-sectional shape is strongly impacted by the presence of the linea aspera, positioned in its typical posterior position, providing an area for the quadriceps and adductor muscles to attach. The early development of the linea aspera is especially influenced by the adductor

magnus muscle (Mittelmeier et al., 1994), which attaches along the medial aspect of the linea aspera. According to Goldman et al. (2009), this is potentially accountable for the posterio-medial drift in young children (up to 8 years old). Adductor magnus and some other muscles develop considerable strength specifically with the onset of walking. Goldman et al. (2009) suggest that this early drift pattern might, in addition, be involved in the achievement of the bicondylar angle, the angle between the long axis of the femoral shaft and a line tangential to the distal aspect of both femoral condyles (in frontal view). This angle is unique to humans and keeps the center of gravity above the knee during bipedal gait. It develops early in life, and is normally complete around age 8 (Tardieu and Damsin, 1997). This, and changes in drift pattern in the femur around age 12 (Goldman et al., 2009), suggest the pattern of lateral modeling drift observed in this study is part of a later developmental stage, however one that is not necessarily disconnected from these early developments. In fact, to account for the bicondylar angle through the adolescent growth spurt, lateral drift could be necessary for a continuous repositioning, specifically of the distal aspect of the element over the knee. This could also, at least partly, explain the differences in drift magnitude we observed along the femoral shaft.

There are other factors that could cause femoral drift area to vary this much along its diaphysis. One phenomenon potentially contributing is that the majority of growth in the femur occurs in the distal femoral growth plate (Pritchett, 1992). This could lend bias toward a younger tissue age in the distal diaphysis, as bone needs to "catch up" with the longitudinal growth and achieve the right balance between diaphyseal length and its cross-sectional diameters. This alone, rather than differential rates of remodeling, could account for larger remnants of primary bone in the distal femoral diaphysis.

Other Considerations and Limitations

Many studies have assessed bone growth, adaptation and ontogenetic diaphyseal changes through macroscopic analyses of cross-sectional geometrics (Ruff and Hayes, 1983; Maggiano et al., 2008; Gosman et al., 2013). This method assumes the diaphysis is a standard beam and calculates moments of area as an indicator of diaphyseal bending rigidity. Geometric cross-sectional studies are most commonly applied to femora, since femoral expansion along the anterio-posterior plane shows a strong relationship to mobility and is therefore frequently used to enhance bioarchaeological interpretations (Ruff and Hayes, 1983; Stock and Pfeiffer, 2004; Marchi et al., 2006; Maggiano et al., 2008). Greater expansions in the anterio-posterior plane, as characteristic for highly mobile populations, could lead to the assumption that this might be the dominant direction of bone modeling and growth. Data presented here and by Goldman et al. (2009) indicate the dominant drift direction in the femur is not anterio-posterior, but lateral. Accordingly, Goldman and colleagues suggest that modeling drift patterning appears to predate changes in geometric properties of the cross-section. However, discrepancies between cross-sectional shape and the regional distribution of primary lamellar bone could indicate that the mechanical adaptation to activity-related bending forces and bone

modeling drift are not responsive to the same scale or stimuli nor affect the same scale of boney response. Studies differentiating the inputs on bone morphology, e.g. the demands imposed on the bone that are encountered early in life, even before the onset of adult behaviors or rapid adolescent growth, are necessary to reveal hidden and useful variation in bone growth and mechanical adaptation across or between populations.

Another important side-effect of modeling drift that has not been addressed adequately in the literature is that drift causes discrete and potentially adjacent tissues within the diaphysis to have different tissue ages (Wu et al., 1970). It is important to recognize that due to drift, large expanses of bone or even an entire side of the diaphyseal cortex could be comprised of tissue from one or even two decades older than adjacent regions or opposing cortices (Enlow, 1962; Maggiano, 2012b). Tissue age variation is specifically interesting in the femur for two reasons. First, it is the most histologically well-known bone and is used in many applied methods. Second, tissue type varies not only within its cross-section (Iwaniec et al., 1998; Chan et al., 2007) but, as shown in the present study, along its shaft. This means that, within an individual, tissue age could be significantly different between a proximal and a distal sample from the same ROI. In this study the maximal gap in age difference could approach up to 45 years, but other studies suggest individuals as old as 90 might still display endosteal tissues consistent with drift phenomena described here (Tim Gocha, personal communication). This circumstance calls for caution especially for age related histological analyses. Other types of histological examinations could benefit from taking modeling drift and tissue-age into account, including establishing estimates of effective age of adult compacta for bones other than the rib, spatial analysis of microfractures, osteocyte lacunar density, osteon circularity and bone porosity. Varying tissue age could even affect results from stable isotopic or other chemical bone analysis (Maggiano and White, 2013). A more complete understanding of modeling drift could potentially improve statistical strength of histomorphometric comparisons in many applications.

This study shows that regional variation in primary tissue deposition and microstructural variation are valuable tools for the reconstruction of modeling drift and essential for a better understanding of bone growth and adaptation. Using more than one cross-sectional location along the diaphysis has brought to light important details about humeral and femoral drift, which otherwise would remain unknown. While midshaft cross-sections are sufficient to gain information about general drift directions and magnitudes, additional longitudinal sections permit a much more detailed interpretation and are essential to an improved understanding of modeling drift. The application of the starburst point-count technique in this study captured regional variations in tissue distribution sufficient for statistical analysis, and confirmed previously reported modeling drift patterns (deriving from qualitative or cortical surface techniques) (Goldman et al., 2009; Maggiano et al., 2011). One limitation of our study and its comparability with others is the lack of a standardized method for the determination of anatomical axes on dry bone. Convention in femoral cross-sectional analyses is to use the linea aspera as the posterior indicator. Likewise, in the humerus, a

convention similar to the one described in our methods section could be set. Studies on directionality of tissue distributions would benefit greatly from a more detailed understanding of dry-bone versus physiological anatomical axes to aid standardization. This study also consists of a relatively small sample and certainly obscures important variation due to innumerable factors (i.e., age, sex, activity level, species). Larger scale analyses are underway in several populations adding specific detail to the more widely applicable trends discussed here. This research demonstrates both, the significance and complexity of interrelations among bone growth, modeling, and modeling drift and encourages further study, benefitting efforts in bioarchaeology and anatomy by increasing our understanding of morphological change during bone growth and adaptation.

ACKNOWLEDGEMENTS

LITERATURE CITED

Aiello L, Dean C. 2002. An introduction to human evolutionary anatomy. New York: Academic Press.

Cambra-Moo O, Meneses CN, Rodríguez Barbero MA, García Gil O, Rascón Pérez J, Rello-Varona S, Campo Martín M, González Martín A. 2012. Mapping human long bone compartmentalisation during ontogeny: A new methodological approach. J Stuct Biol 178:338–349.

Cambra-Moo O, Meneses CN, Rodríguez Barbero MA, García Gil O, Rascón Pérez J, Rello-Varona S, D'Angelo M, Campo Martín M, González Martín A. 2014. An approach to the histomorphological and histochemical variations of the humerus cortical bone through human ontogeny. J Anat 224:634–646.

Carpenter RD, Carter DR. 2008. The mechanobiological effects of periosteal surface loads. Biomech Model Mechanobiol 7:227–242.

Chan AH, Crowder CM, Rogers TL. 2007. Variation in cortical bone histology within the human femur and its impact on estimating age at death. Am J Phys Anthropol 132:80–88.

Chi-Keb JR, Albertos-González VM, Ortega-Munoz A, Tiesler VG. 2013. A new reference collection of documented human skeletons from Mérida, Yucatan, Mexico. Homo 64:366–376.

Currey JD. 2003. The many adaptation of bone. J Biomech 36:1487–1495.

Edelson G. 2000. The development of humeral head retroversion. J Shoulder Elbow Surg 9:316–318.

Enlow D. 1962. A study of the postnatal growth and remodeling of bone. Am J Anat 110:79–101.

Frost H. 1973. Bone modeling and skeletal modeling errors. Orthopaedic Lectures Volume IV. Springfield: Charles C. Thomas.

Goldman H, Thomas CDL, Clement JG, Bromage TG. 2005. Relationships among microstructural porperties of bone at the human femur. J Anat 206:127–139.

Goldman HM, McFarlin SC, Cooper DMI, Thomas CDL, Clement JG. 2009. Ontogenetic patterning of cortical bone microstructure and geometry at the human mid-shaft femur. Anat Rec 292:24–64.

Gosman JH, Hubbell ZR, Shaw CN, Ryan TM. 2013. Development of cortical bone geometry in the human femoral and tibial diaphysis. Anat Rec 296:774–787.

Gross TS, Srinivasan S, Liu CC, Clemens TL, Bain SD. 2002. Non-invasive loading of the murine tibia: an in vivo model for the study of mechanotransduction. J Bone Min Res 17:493–501.

Hawkey DE, Merbs CF. 1995. Activity-induced musculoskeletal stress markers (MSM) and subsistence strategy changes among ancient Hudson Bay Eskimos. Int J Osteoarchaeol 5:324–338.

Hoyte DAN, Enlow DH. 1966. Wolff's law and the problem of muscle attachment on resorptive surfaces of bone. Am J Phys Anthropol 24:205–213.

Iwaniec UT, Crenshaw TD, Schoeninger MJ, Stout SD, Ericksen MF. 1998. Methods for improving the efficiency of estimating total density in the human anterior mid-diaphyseal femur. Am J Phys Anthropol 107:13–24.

Jones DB, Nolte H, Scholuebbers JG, Turner E, Veltel D. 1991. Biochemical signal transduction of mechanical stain in osteoblast-like cells. Biomaterials 12:101–110.

Krahl VE, Evans FG. 1945. Humeral torsion in man. Am J Phys Anthropol 3:229–253.

Maggiano CM. 2012a. Histomorphometry of humeral primary bone: evaluating the endosteal lamellar pocket as an indicator of modeling drift in archaeological and modern skeletal samples. Columbus: The Ohio State University. PhD Thesis.

Maggiano CM. 2012b. Making the mold: A microstructural perspective on bone modeling during growth and mechanical adaptation. In: Stout S, Crowder C, editors. Hard tissue histology: An anthropological perspective. Boca Raton: CRC Press. p 45–90.

Maggiano CM, Maggiano IS, Tiesler VG, Chi-Keb JR, Stout SD. In press. Methods and theory in bone modeling drift: Comparing spatial analyses of primary bone distributions in the human humerus. J Anat.

Maggiano CM, White C. 2013. New potential for collecting developmental and seasonal dietary, mobility, and climate data from ancient human long bones: High spatial resolution stable isotopic analysis and the endosteal lamellar pocket. Am J Phys Anthropol 105.

Maggiano IS, Maggiano CM, Tiesler V, Kierdorf H, Stout SD, Schultz M. 2011. A distinct region of microarchitectural variation in femoral compact bone: Histomorphology of the endosteal lamellar pocket. Int J Osteoarch 21:743–750.

Maggiano IS, Schultz M, Kierdorf H, Sosa TS, Maggiano CM, Tiesler Blos V. 2008. Cross-sectional analysis of long bones, occupational activities and long-distance trade of the Classic Maya from Xcambó – Archaeological and osteological evidence. Am J Phys Anthrop 136:470–477.

Marchi D, Sparacello VS, Holt BM, Formicola V. 2006. Biomechanical approach to the reconstruction of activity patterns in Neolithic Western Liguria, Italy. Am J Phys Anthrop 131:447–455.

Martin RB, Burr DB, Sharkey NA. 1998. Skeletal tissue mechanics. New York: Springer.

McFarlin SC, Terranova CJ, Zihlman AL, Enlow DH, Bromage TG. 2008. Regional variability in secondary remodeling within long bone cortices of catarrhine primates: The influence of bone growth history. J Anat 213:308–324.

Meade JB, Cowin SC, Klawitter JJ, van Buskirk WC, Skinner HB. 1984. Bone remodeling due to continuously applied loads. Calcif Tiss Int 36:S25–S30.

Mittelmeier T, Mattheck C, Dietrich F. 1994. Effects of mechanical loading on the profile of human femoral diaphyseal geometry. Med Eng Phys 16:75–81.

Molnar P. 2006. Tracing prehistoric activities: musculoskeletal stress marker analysis of a stone-age population on the island of Gotland in the Baltic sea. Am J Phys Anthropol 129:12–23.

Mosley JR, March BM, Lynch J, Lanyon LE. 1997. Strain magnitude related changes in whole bone architecture in growing rats. Bone 20:191–198.

Mosley JR, Lanyon LE. 1998. Strain rate as a controlling influence on adaptive modeling in response to dynamic loading of the ulna in growing male rats. Bone 23:313–318.

Mosley JR, Lanyon LE. 2002. Growth rate rather than gender determines the size of the adaptive response of the growing skeleton to mechanical strain. Bone 30:314–319.

Paine RR, Godfrey LR. 1997. The scaling of skeletal microanatomy in non-human primates. J Zool London 241:803–821.

Parfitt AM. 1983. The physiologic and clinical significance of bone histomorphometric data. In: Recker RR, editor. Bone Histomorphometry: Techniques and Interpretation. Boca Raton, CRC Press. p.143–244.

Parfitt AM. 2000. The mechanism of coupling: a role for the vasculature. Bone 26:319–323.

Pritchett J. 1992. Longitudinal growth and growth-plate activity in the lower extremity. Clin Orthop Rel Res 275:274–279.

Robling AD, Duijvelaar KM, Geevers JV, Ohashi N, Turner CH. 2001. Modulation of appositional and longitudinal bone growth in the rat ulna by applied static and dynamic force. Bone 29:105–113.

Ruff CMomentMacroJ program [internet]. Available at: http://www.hopkinsmedicine.org/fae/mmacro.htm

Ruff C, Hayes W. 1983. Cross-sectional geometry of Pecos Pueblo femora and tibiae—a biomechanical investigation. I. Method and general patterns of variation. Am J Phys Anthropol 60:359–381.

Schlecht SH. 2012. A histomorphometric analysis of muscular insertion regions: understanding enthesis etiology. Columbus, The Ohio State University. PhD Dissertation.

Schultz M. 1988. Methoden der Licht- und Elektronenmikroskopie. In: Knussmann R, editor: Handbuch der vergleichenden Biologie des Menschen 1, 1. Stuttgart: G. Fischer. p 698–730.

Schultz M, Drommer R. 1983. Möglichkeiten der Präparateherstellung aus dem Gesichtsschädelbereich für die makroskopische und mikroskopische Untersuchung unter Verwendung neuer Kunststofftechniken. In: Hoppe WG, editor. Fortschritte der Kiefer- und Gesichts-Chirurgie 28. Experimentelle Mund-Kiefer-Gesichts-Chirurgie. Mikrochirurgische Eingriffe. Stuttgart: G. Thieme. p.95-97.

Stock J, Pfeiffer S. 2004. Long bone robusticity and subsistence behaviour among later Stone Age foragers of the forest and fynbos biomes of South Africa. J Archaeol Sci 31:999–1013.

Tardieu C, Damsin JP. 1997. Evolution of the angle of obliquity of the femoral diaphysis during growth-correlations. Surg Radiol Anat 19:91–97.

Taylor RE, Zheng C, Jackson RP, Doll JC, Chen JC, Holzbaur KRC, Besierd T, Kuhl E. 2009. The phenomenon of twisted growth: humeral torsion in dominant arms of high performance tennis players. Comp Meth Biomech Biomed Engineering: 12:83–93.

Turner CH. 1998. Three rules for bone adaptation to mechanical stimuli. Bone 23:399–407.

Whiteley RJ, Ginn KA, Nicholson LL, Adams RD. 2009. Sports participation and humeral torsion. Journal of Orthopaedic and Sports Physical Therapy 39:256–259.

Wu K, Schubeck K, Frost H, Villanueva A. 1970. Haversian bone formation rates determined by a new method in a mastodon, and in human Diabetes Mellitus and Osteoporosis. Calcif Tiss Res 6: 204–219.